M R S Internet Journal Nitride Semiconductor Research

On the Bandstructure in GaInN/GaN Heterostructures - Strain, Band Gap and Piezoelectric Effect

Christian Wetzel[1], Shugo Nitta[1], Tetsuya Takeuchi[1], Shigeo Yamaguchi[1], H. Amano[1] and I. Akasaki[1]

[1]*Department of Electrical and Electronic Engineering, Meijo University*,

(Received Friday, August 28, 1998; accepted Tuesday, October 6, 1998)

A study of the optoelectronic properties of strained 40 nm $Ga_{1-x}In_xN$ layers on GaN films is presented. The fact of pseudomorphic strain leads to a new interpretation of the film composition when derived from x-ray scattering. In addition we directly confirm that strain induces huge piezoelectric fields in this uniaxial system by the observation of Franz-Keldysh oscillations in photoreflection. As a function of composition ($0 < x < 0.2$) and strain we derive the electronic band gap energy and the piezoelectric field strength. We interpret both in terms of effective bowing parameters and piezoelectric coefficients, respectively. From a spatially resolved micro photoluminescence at room temperature we find no evidence for spatial band gap or composition variations of more than 60 meV over the length scale from 1 to 50 μm (x=0.187) in our material. At the same time, an observed discrepancy between photoluminescence peak energy and photoreflection band gap energy increases with x to some 160 meV. We attribute this redshift to photon assisted tunneling in the huge piezoelectric fields (Franz-Keldysh effect).

1 Introduction

Significant progress in the hetero-epitaxy of group-III nitrides [1] using low temperature deposited buffer layers [2] [3] [4], multiple buffer layer techniques [5] and lateral epitaxial overgrowth [6] have led to record breaking devices such as light emitting diodes and laser diodes [7] [8] in the UV, blue and green region as well as high frequency [9] and high power [10] switching devices. As a function of composition the alloys of GaN and InN should cover the entire spectral region from the very near UV to the red while AlGaN covers a wide range in the near UV. In detail, however, significant controversy exists about the compositional dependence of the electronic band gap in $Ga_{1-x}In_xN$ and its heterostructures with, i.e., GaN (see. e.g. Refs. [11] [12]). Comparing electro- and photoluminescence results with photo voltage and electroabsorption data Chichibu *et al*. [13] [14] [15] find significant discrepancies in the band gap energy between absorption and emission energies amounting to some 100 to 300 meV. It has been proposed that this effect should be correlated with the difficulty to homogeneously incorporate high InN fractions during layer growth [16] [17] [14] [15]. Indeed inhomogeneous luminescence and structural properties as revealed by spatially resolved experiments [16] [17] [18] have been reported to find grain-like features that could define areas of variable band gap energy. In the extreme case large electric dipole moments in quantum dot-like features [19] could result in high optical gain of the material which should be beneficial for laser device performance [17] [18].

In order to elucidate the optoelectronic properties of GaInN we present our studies of $Ga_{1-x}In_xN$/GaN ($0 < x < 0.2$) single heterostructures by photoreflection (PR), photoluminescence (PL), and spatially resolved PL. Some aspects have in part been published elsewhere [20] [21] [22] [23]. The paper is organized as follows. After this Introduction(Section 1.) we give details on the samples and experiments in Experimental (Section 2.). We will first discuss the Strain and Composition(Section 3.) of our samples based on x-ray diffraction results. We then address the aspects of homogeneity in a Section 4. Spatial Fluctuations, then interpret and discuss PR data in terms of the Electronic Band Gap Energy (Section 5.). We continue with the determination of Piezoelectric Fields (Section 6.) and interpret it in terms of Piezoelectric Constants (Section .7). This leads to an interpretation of the Luminescence

https://doi.org/10.1557/S1092578300001034 Published online by Cambridge University Press

Band Gap in Section .8 and conclude in Section 9. Conclusions.

2 Experimental

Single $Ga_{1-x}In_xN$/GaN heterostructures with an InN fraction x in the range of $0 < x < 0.2$ were studied. Samples were grown in metal organic vapor phase epitaxy (MOVPE) on (0001) sapphire substrates using low temperature deposited AlN buffer layers [24] [25]. Further details have been given in Ref. [22]. Ternary layers at a thickness of 40 nm were grown pseudomorphically onto 2 μm GaN. Pseudomorphic growth and x were determined from high resolution x-ray diffraction of a and c lattice constants [25]. PR at room temperature was performed using a Xe-arc lamp source in near-to-perpendicular reflection. Periodic photomodulation was performed using a 40 mW 325 nm HeCd Laser. The AC signal component was normalized to the DC signal forming $\Delta R/R$. The phase was fixed to the phase of the PL. Macroscopic PL under identical conditions was performed using the same laser. Micro PL was performed with 20 mW of a 325 nm laser focused to a spot size of 1 μm^2 and confocal microscope collection. Automated spatial mapping of micro PL was performed using an x-y stage and sequential acquisition.

3 Strain and Composition

Due to the lattice mismatch of GaN and InN large strain is induced in the epitaxial layer system at the heterointerfaces of GaInN and GaN. Using the theoretical models of Fischer *et al*. [26] and Matthews and Blakeslee [27] that have been successful in predicting the conditions, i.e., in GaAsP systems [27] a relaxation of the biaxially compressed layer should occur for critical layer thicknesses of 4 - 14 nm (x=0.1) and 6.3 nm (x=0.2) when room temperature stiffness constants of GaN are applied [24]. Here, however, for all the $Ga_{1-x}In_xN$/GaN samples in the study ($0<x<0.2$) no relaxation can be observed at a ternary film thickness of 40 nm. This has been documented by the line-up of the a-lattice constants of the (2 0 $\bar{2}$ 4) x-ray diffraction maxima in k-space mapping [1]. Consequently a large biaxial compression is maintained throughout the thickness of the GaInN layers. Assuming a linear variation of the lattice constants in unstrained GaInN between the values of GaN and InN and the stiffness constants of GaN c_{13}=11.4 $\times 10^{11}$ dyn/cm^2, c_{33}=38.1 $\times 10^{11}$ dyn/cm^2, derived from Brillouin scattering [28] (for a discussion of the issue of varying stiffness constants see Ref. [29]) we find the following strain conditions as a function of composition x for the unstrained case:

$$c(x) = c_{GaN}\,(1–x) + c_{InN}\;x = 5.184\ \text{Å}\,(1–x) + 5.705\ \text{Å}\,x\,, \qquad (1)$$

$$a(x) = a_{GaN}\,(1–x) + a_{InN}\;x = 3.188\ \text{Å}\,(1–x) + 3.540\ \text{Å}\,x\,. \qquad (2)$$

This dependence and the following discussions are based on the assumed validity of Vegard's law for the interpolation of the lattice parameter from the binaries for strain-free material [30] [a] . We refer our data to the strain condition of the 2 μm epitaxial GaN layer underneath the ternary film where we obtain c_1= 5.189 Å, a_1= 3.182 Å and derive strain values $\varepsilon_{xx} = a_1/a_x - 1 < 0$, and, as a consequence within Hook's law, $\varepsilon_{zz} = c_1/c_x - 1 = -2\ c_{13}/c_{33}\ \varepsilon_{xx} > 0$. For x = 0.2 we therefore induce strain ε_{zz} = 0.015, ε_{xx} = -0.023. For comparison in epitaxial GaN films strain values up to ε_{zz} = 0.0012 are obtained depending on substrate and growth technique [31].

For the pseudomorphically strained case we consequently derive

$$a = 3.182\ \text{Å}\,, \qquad (3)$$

$$x = 1.165\,(c/\text{Å}–5.184)\,[1–0.16(c/\text{Å}–5.184)] – 0.01, \qquad (4)$$

where the last offset term results from the strained conditions of the GaN epilayer [20]. The deformation of the unit cell therefore significantly affects the interpretation of the InN fraction from c-lattice constants in x-ray diffraction [22]. Neglecting the strain conditions results in a overestimated composition x' with

$$x = 0.62\,x' – 0.059x'^2. \qquad (5)$$

Many composition values cited in the literature are therefore likely to overestimate x by roughly a factor of 2. At present we are not aware of any model that could explain the large thicknesses of the unrelaxed layers. We tentatively assign this observation to the fact of a higher degree of ionicity contributing in the bonding forces in the nitrides [20] and the uncertainties of the stiffness constants at the growth temperature.

4 Spatial Fluctuations

Several groups reported the observation of a spatial variation in the contrast of transmission [16] and scanning electron microscopy images [32] of GaInN layers as well as in the cathodoluminescence intensity [17]. In part these effects have been attributed to compositional fluctuations [17] exceeding the degree of typical alloy fluctuations. Indeed In-rich areas or islands could result in locations of lower band gap enhancing radiative emission by localizing the carriers and possible enhancement of wave function overlap [19] [33]. In these cathode-ray experiments care must be taken to avoid possible strong effect by the observation itself.

https://doi.org/10.1557/S1092578300001034 Published online by Cambridge University Press

Radiation damage has been proposed to alter the conditions of the sample and possibly create contrast upon observation [34] [35]. Annealing experiments of GaInN have shown that In-rich regions can be formed by heating [36].

In x-ray diffraction of GaInN composition series the appearance of multiple extrema has been attributed to the coexistence of distinct alloy compositions [31] [37]. Theory indeed predicts regimes of growth conditions under which a phase separation of alloys of different composition should occur [38]. According to these results, a large and symmetric separation into phases with x_1=y and x_2=1-y should be expected under equilibrium conditions. Under epitaxial non-equilibrium growth conditions typical for MOVPE, however, it should be possible to stabilize films of homogeneous composition $x \leq 0.20$ [34].

In order to identify the role of possible fluctuations and their contribution to the emission process we performed a spatially resolved PL mapping (T=300 K) covering an area of 50 ×50 μm^2 at a 1 μm^2 resolution defined by the UV excitation laser spot [21]. For a $Ga_{1-x}In_xN$/GaN, x=0.187, single heterostructure the peak energy of the PL maximum is shown in Figure 1a). (The energy scale is color-coded from dark red to white). The respective peak intensity is shown in Figure 1b) on a logarithmic scale. A spatial fluctuation of the peak energy is readily observed with a total energetical variation of 40 – 60 meV.

For the ease of visual interpretation a portion of the intensity image has been arranged next to the corresponding peak energy data and flipped around the y-axis. In this presentation the high symmetry of both values becomes obvious. Apparently areas of lower emission energy only contribute with a smaller intensity. States of lower transition energy are therefore not preferred in the emission process over states with higher energy.

Figure 2 represents a statistical analysis of this data. The peak energy centers at 2.615 eV with a halfwidth of 25 meV (Figure 2a). A low energy shoulder extends for 50 meV. However, weighing these peak positions with their respective intensity these low energy contributions are strongly suppressed and the high energy parts are enhanced. This clearly indicates that luminescence originating in states below the main transition energy do not significantly contribute in the emission process. Instead the dominant transition appears with a very narrow linewidth of 28 meV (Figure 2b).

The emission linewidth in every pixel, however, can be as large as 160 meV and is significantly larger. The different halfwidth in the emission spectra and the variation of the peak energy indicates that spatial fluctuation on the length scale 1 - 50 μm is not the origin of the broad PL line. The fact that samples can be obtained that show this narrow distribution of the PL gap energy indicates that observed broader variations are not impossible to overcome and that they are most likely induced by an instability in the growth process rather than by insurmountable disorder or ordering effects in $Ga_{1-x}In_xN$/GaN, x=0.187. In this material we therefore have no indication that the formation of quantum dots in In-rich regions plays a significant role in the dominant light emission process.

5 Electronic Band Gap Energy (0<x<0.2)

The problem in the description of the radiative emission process is accompanied by an uncertainty of the compositional dependence of the band gap energy. To this end we performed PR spectroscopy on thin layer structures (T=300 K). Figure 3 represents the arbitrarily scaled PR signal ΔR/R in the sequence of composition. In all the spectra a sharp and narrow signal is seen at 3.42 eV marking the excitonic band gap in GaN underneath the ternary layer. This narrow signal with linewidths of 10-20 meV contrasts to a significantly broader signal at lower energies assigned to the band gap in GaInN. The large oscillation period indicates a strong interaction of a continuum of states with a second partner state [39]. The continuos nature of the signal and additional extrema on the high energy side strongly indicate that this signal are Franz-Keldysh oscillations at the band gap in the presence of a large electric field F [40] [23]. The interaction partner therefore is the same continuum of states separated in real space by Δx and shifted in energy by $\Delta E = F e \Delta x$. Figure 4 gives a schematic of the bandstructure in the presence of an electric field. Tilting the bandstructure in real space by applying a field F electrons in the conduction band are reflected at the barrier formed by the forbidden band gap. Considering a specific location of an interband transition indicated by the red line a fixed phase correlation is established between the wave functions of the previously free electrons with respect to energy. In the result an oscillatory behavior is observed in the density of states in the vicinity of the band gap. Taking into account the full dispersion at the bandedge in three dimensions Aspnes has given a description of the PR signal in terms of the electro-optical functions [41] [42] [b] . Oscillations are not limited to energies above the band gap. Instead interference occurs as well with the evanescent part of the wave functions tunneling into the band gap. From comparison with the electro-optical functions the DOS band gap energy lies close to the overall PR minimum. Due to the high symmetry of the

https://doi.org/10.1557/S1092578300001034 Published online by Cambridge University Press

oscillation we assign the PR band gap to this minimum energy [22] [40].

The resulting values can be best described by an interpolation of the energies in the binaries considering an effective bowing parameter b in [20] [22]:

$$E_g = 3.42\ \text{eV}\ (1-x) + 1.89\ \text{eV}\ x - b\ x\ (1-x)\ . \qquad (6)$$

Here we use the band gap energies of the epitaxial GaN layer and the literature value for InN [43]. Within the range $0 < x < 0.2$ we find a good description for b=2.6 eV [22] in this absorption-type PR band gap. PL data finds smaller values for the effective emission band gap and the data can be well described assuming b=3.2 eV [24] [22].

The strain-free condition can be extrapolated from the above data using the experimental band gap deformation potential of GaN $\partial E_{gap}/\partial \varepsilon_{zz}$ =15.4 eV [31]. In the result b=3.8 eV is found for the DOS band gap in strain-free $Ga_{1-x}In_xN$, $0<x<0.2$ [22]. This perfectly agrees with a recent absorption study by McCluskey *et al*. [44] finding b=3.8 eV for x=0.1. First principles calculations by several groups, however, find that the bowing parameter should vary significantly with composition, i.e. b = {4.8, 3.5, 3.0} eV for x = {0.0525, 0.125, 0.25}, respectively (For details see Ref. [22]).

The above finding is based on the composition determination described in Chapter 3. Strain and Composition. Neglecting the pseudomorphic strain conditions and using x' values instead the PR data would be best described by b=0.9 eV. This value is close to the data found by Nakamura *et al*. [45] [46] [47] described by b = 1 eV. The earlier results by Osamura *et al*. [32] finding b=1 eV is based on a single parameter fit to data covering the entire composition range. Three PL data points falling in the x-range considered here are in fact better described by our value of b=3.2 eV [22].

6 Piezoelectric Fields

The PR oscillations exhibit several side extrema on the high energy side (Figure 5). The field is proportional to the main oscillation period to the power of 3/2 and therefore varies faster than the period itself. An interpretation of the oscillation period according to Aspnes [41] [42] [48] allows for a determination of the electro-optical energy and the strength of the electric field across the ternary layer [23]. In this direct determination the only material parameter is the joined DOS effective mass assumed to be fixed at the GaN value of $m^*=0.2\ m_e$ [49]. Field values up to a maximum of 1.12 MV/cm are observed. The large value of the field and its insensitivity to the modulation intensity indicate that this field is not induced by the photogenerated carriers. Instead it is a constant field present in the structure and we assign it to the piezoelectric field induced by the heteroepitaxial strain along the z-axis.

Figure 6 depicts the field values as a function of the applied heteroepitaxial strain. We observe a clear trend towards larger fields for increased strain. The observed sample-to-sample scatter is well beyond the statistical error of the experiment. The field increases at an average differential slope $\partial F/\partial \varepsilon_{zz}$=3.4 - 3.7 $\times 10^9$ V/m. In addition the majority of samples exhibits an offset behavior that corresponds to a strain-free polarization of P=3.7 $\times 10^{-3}$ C/m^2. Note that neither direction nor sign of the electric field can be determined directly in these experiments without assumptions of the photoscreening mechanism. Franz-Keldysh oscillations are governed by the largest field component assumed here to lie in z-direction. The observed offset behavior, however, indicates that strain-free polarization and strain induced polarization are of opposite sign. Some samples do not show this retardation effect and exhibit significantly higher field values peaking in F=1.12 MV/cm for ε_{zz}=3.2 %, x=0.18. This field corresponds to a large effective piezoelectric charge density of 6.4 $\times 10^{12}$ cm^{-2} confined to a δ-layer at the interfaces. The offset behavior therefore suggests that it is produced by an apparent relaxation in piezoelectric polarization. This relaxation is not accompanied by a strain relaxation that would be observable in x-ray diffraction. We tentatively assign this process in part to screening by mobile carriers and the generation of structural defects suitable to compensate the piezoelectric fields such as inversion domains.

Takeuchi *et al*. [50] [51] studied the bias voltage dependence of the photoluminescence in GaInN/GaN multiple quantum well device structures on both, sapphire and 6H-SiC substrate. Under a variation of the bias voltage across the structure the quantum confined Stark effect was demonstrated. From the blue shift of the PL under reverse bias the piezoelectric field was found to have the opposite direction than the bias field which points from the *n*-layer on the substrate side to the *p*-layer on the growth surface side. In these MOVPE structures biaxial compression ($\varepsilon_{xx}<0$, $\varepsilon_{zz}>0$) of the well layer therefore induces a downward slope in energy of the bandedges towards the growth surface between the fixed piezoelectric charges. A schematic of the distribution and fixed piezoelectric charges together with the resulting fields and bandedge structure in an undoped double heterostructure is shown in Figure 7.

7 Piezoelectric Constants

The polarization P of the heterostructure sample is the sum of an equilibrium polarization P_{eq} (also somewhat misleadingly labeled spontaneous polarization) in the non-centrosymmetric structure in this partially ionic

https://doi.org/10.1557/S1092578300001034 Published online by Cambridge University Press

material and contributions from partial derivatives with respect to temperature $\partial P/\partial T$, composition $\partial P/\partial x$, strain $\partial P/\partial \varepsilon$ as well as their spatial derivatives, electronic response effects like screening of mobile carriers and macroscopic contributions of surface terminations, charges, contaminations and applied voltages P_{ex}. $\partial P/\partial T\, \delta x$ is referred to as the pyroelectric component, which historically also labels the total polarization . $\partial P/\partial \varepsilon\, \delta\varepsilon$ is the piezoelectric component.

In thermodynamic equilibrium the inner polarization is balanced macroscopically by external fixed charges leading to vanishing F in homogenous layers. This is equivalent to a shortcut between the surfaces. At the GaN-GaInN heterointerface, however, fields may exist locally the strength of which is given by

$$\epsilon_0\epsilon_r F_z = P_{z,GaInN} - P_{z,GaN} = \Delta P_z = \frac{\partial P_z}{\partial x}\delta x + \frac{\partial P_z}{\partial \epsilon_{zz}}\delta\epsilon_{zz}, \quad (7)$$

In the above experiment we can not distinguish contributions $\partial P/\partial \varepsilon$ and $\partial P/\partial x$. Due to the similar ratio c/a of the lattice constants in GaN and InN we attribute the field entirely due to the piezoelectric component, $\partial P/\partial\epsilon \gg \partial P/\partial x$.

In wurtzite the piezoelectric polarization along the z-axis is given by

$$P_z = e_{31}(\varepsilon_{xx} + \varepsilon_{yy}) + e_{33}\varepsilon_{zz}, \quad (8)$$

where e_{31} and e_{33} are components of the piezoelectric tensor. Assuming a constant dielectric coefficient ε_r=10.4 at the value of GaN and $\varepsilon_{xx}=\varepsilon_{yy}=-\varepsilon_{zz}$ c_{33}/c_{13} we experimentally find

$$e_{33} - 3.34\, e_{31} = 0.3\ \mathrm{C/m^2}. \quad (9)$$

In order to compare with literature data we continue with the quasi-cubic approximation where $P_{zz} = 3^{-1/2} e_{14}(2+c_{33}/c_{13})\varepsilon_{zz}$ holds resulting in

$$e_{14} = 0.1 \pm 0.01\ \mathrm{C/m^2}. \quad (10)$$

This value is significantly smaller than the value obtained by Bykhovski *et al.* [52] in piezoresistivity experiments e_{14}=0.56 C/m^2. Our value, however, is significantly closer to the trend of the piezoelectric coefficient e_{14} in other III-V and II-VI (Figure 8, after Shur [53]).

Bernardini, Fiorentini and Vanderbilt [54] recently performed first principles calculations of the piezoelectric properties in the nitrides and derived the piezoelectric coefficients and values for the equilibrium polarization. Indeed, the equilibrium polarization of GaN and InN is found to vary by only 10 % justifying our above approximation to neglect the composition effects in the equilibrium polarization. For GaN they predict values of P_{eq}=-29 $\times 10^{-3}$ C/m^2 and $\delta P/\delta\, \varepsilon_{zz}$=2.37 C/m^2, equivalent to e_{14} = 0.79 C/m^2. These values are higher by a factor of eight compared to our values but compare better with the results of Bykhovski *et al.* [52] (Figure 8). Quantitative discrepancies of theoretical and experimental piezoelectric coefficients have also been obtained in other compound materials [55]. These large piezoelectric charges come in pairs of positively and negatively charged layers and form a perfectly periodic single delta doping layer. The strained induced areal charge density of

$$\partial N/\partial\varepsilon_{zz} = 1.9 \times 10^{14}\ \mathrm{cm^{-2}} \quad \text{and} \quad (11)$$

$$\partial N/\partial x = 3.4 \times 10^{13}\ \mathrm{cm^{-2}} \quad (12)$$

correspond to

$$N = 6.8 \times 10^{12}\ \mathrm{cm^{-2}} \quad \text{for} \quad x=0.2. \quad (13)$$

Doping and screening effects therefore are negligible unless charge densities reach similar large values. The accumulations of such a huge charge density is of significant relevance for high power devices.

8 Luminescence Band Gap

The maximum of the PL in the vicinity of the band gap appears to be redshifted with respect to the absorption DOS band gap derived in the PR experiment. Figure 9 gives pairs of PL and PR in the 40 nm single heterostructures (see Ref [23] for a detailed analysis). Varying with composition the redshift can be as large as 110 - 160 meV. Similar values between PL and absorption-type photovoltage wave been reported by Chichibu *et al.* on thin film heterostructures [13] [14]. The PL linewidths amount to about the same high values (note that at the same time the variation of the weighed *peak* energy in the spatial mapping (Chapter 4.) can be as small as 28 meV). The redshift approximately corresponds to one halfperiod of the Franz-Keldysh oscillation near the band gap. We therefore attribute this redshift to the Franz-Keldysh effect [23]. Spatially indirect transitions across the band gap appear at lower energy due to the tilting of the bands. At the same time the transition probability is reduced exponentially as the area under the triangular tunneling barrier grows without involving impurity or defect states (see schematic in Figure 4):

$$T \approx \exp\left[-\frac{4}{3}\sqrt{\frac{2m*}{\hbar^2}}\frac{(E_g - E)^{3/2}}{eF}\right] \quad (14)$$

https://doi.org/10.1557/S1092578300001034 Published online by Cambridge University Press

Within a halfperiod of the first Franz-Keldysh oscillation $\Delta E = (3\pi/4)^{2/3}(e\hbar F)^{2/3}(2m*)^{-1/3}$ the transition probability has decayed to 4 % of its value at the DOS band gap [23]. In this framework initial and final states are states of delocalized carriers. The exponential "tail" is not induced by any disorder or impurities but rather by the tunneling process in the tilted bandstructure. Additional smaller contributions induced by disorder and impurities are not ruled out. It is our claim, however, that the dominant contribution results from the tunneling process in the electric field [40] [20] [23]. It should be mentioned that in quantum well structures were size quantization is significant this bulk effect is not expected to contribute. Instead due to the finite well width and spatial separation of electrons and holes a redshift is induced by the quantum confined Stark effect as demonstrated by Takeuchi et al. [50] [51].

9 Conclusions

In conclusion we have presented a basis aiming at a consistent interpretation of the optoelectronic properties of strained GaInN layers on GaN films. In order to account for the surprising pseudomorphic strain conditions in thick $Ga_{1-x}In_xN$ films on GaN we have given a relation between composition and lattice parameters. By means of photoreflection spectroscopy we have derived the optical DOS band gap energy as a function of composition in the range of $0 \leq x < 0.2$ and strain. We have derived effective bowing parameters and have been able to explain other results in the literature. We suggest that a number of quoted x compositions given in the literature overestimate the true composition by a factor of two. We have identified and directly determined the strength of huge electric fields in the strained layers and have related them to the piezoelectric properties of the system. From a set of differently strained layers we derived the piezoelectric coefficient which is in reasonable range of other compound systems, but significantly smaller than recent theory values. In order to address recent proposals of a significance of large spatial composition fluctuations in $Ga_{1-x}In_xN$ we have performed a spatially resolved PL analysis and for x=0.187 we find that such effects are well within the range of alloy fluctuation observed in other systems, and concepts of quantum dot formation are not apparent in our material.

Instead we have shown that discrepancies in the PL emission energy and the DOS band gap energy are well explained in the concept of photon assisted tunneling across real space in the huge piezoelectric fields. This study in thin GaInN films has important implications for GaInN/GaN heterostructures as discussed in [20] [21] [56] and other strained nitride layers and heterostructures. Altogether we are convinced that the above developed framework will help to elucidate the exiting properties of group-III nitride heterostructures and lead to a number of new important devices.

ACKNOWLEDGMENTS

This work was partly supported by the Ministry of Education, Science, Sports and Culture of Japan (contract nos.09450133 and 09875083, and High-Tech Research Center Project) and JSPS Research for the Future Program in the Area of Atomic Scale Surface and Interface Dynamics under the project of Dynamic Process and Control of the Buffer Layer at the Interface in a Highly-Mismatched System.

REFERENCES

[a] Deviations form this succesful rule have been proposed by Bellaiche and Zunger [30]. In their model the large bondlength mismatch of the binary constituents should lead to short range ordering. Within the range of our data we do not observe any abrupt variations and effects of the above type are therefore expected to contribute in the large bowing parameter of the band gap energy

[b] Note recent considerations have led to exchange the role of the electrooptic functions F(η) and G(η)

[1] I Akasaki, H Amano, *Jpn. J. Appl. Phys.* ***36***, 5393 (1997).

[2] H. Amano, N. Sawaki, I. Akasaki , Y. Toyoda , *Appl. Phys. Lett.* ***48***, 353-355 (1986).

[3] I. Akasaki, H. Amano, Y. Koide, K. Hiramatsu, N. Sawaki, *J. Cryst. Growth* ***98***, 209 (1989).

[4] I. Akasaki, N. Sawaki, K. Hiramatsu, H. Goto. Report of Priority Area Research Program, supp. by Ministry of Edu. Sci. Culture of Jap (in japanese) (1988) p.106 ff

[5] M Iwaya, T Takeuchi, S Yamaguchi, C Wetzel, H Amano, I Akasaki, *Jpn. J. Appl. Phys.* ***37***, L316 (1998).

[6] D. Kapolnek, S. Keller, R. Vetury, R.D. Underwood, P. Kozodoy, S.P. DenBaars, U.K. Mishra, *Appl. Phys. Lett.* ***71***, 1204-1206 (1997).

[7] S Nakamura, M Senoh, S Nagahama, N Iwasa, T Yamada, T Matsushita, H Kiyoku, Y Sugimoto, *Jpn. J. Appl. Phys.* ***35***, L74-L76 (1996).

[8] I. Akasaki, S. Sota, H. Sakai, T. Tanaka, M. Koike, H. Amano, *Electron. Lett.* ***32***, 1105-1106 (1996).

[9] L. Eastman, K. Chu, W. Schaff, M. Murphy, N Weinmann, T. Eustis, *MRS Internet J. Nitride Semicond. Res.* ***2***, 17 (1997).

[10] Y. -F. Wu, B. P. Keller, S. Keller, D. Kapolnek, S. P. DenBaars, U. K. Mishra, *IEEE Electron Dev. Lett.* ***17***, 455 (1996).

[11] Nitride Semiconductors, Eds. S.P. DenBaars, B.K. Meyer, S. Nakamura, F.A. Ponce, T. Strite, Mater. Res. Soc. Symp. Proc. **482** , 1-1224 (1998)

[12] Proceedings of the Second Int. Conf. on Nitride Semicon. Oct 1997, Tokushima, Japan. J. Cryst. Growth **189/190** , 1-866 (1998)

[13] S. Chichibu, T. Azuhata, T. Sota, S. Nakamura, *Appl. Phys. Lett.* ***69*** , 4188-4190 (1996).

[14] S Chichibu, T Azuhata, T Sata, S Nakamura, *Appl. Phys. Lett.* ***70*** , 2822-2824 (1997).

[15] S. Chichibu, M. Arita, H. Nakanishi, J. Nishio, L. Nishio, Y. Kokuban, K. Itaja, *J. Appl. Phys.* ***83*** , 2860-2862 (1998).

[16] Y. Narukawa, Y. Kawakami, M. Funato, S. Fujita, S. Fujita, S. Nakamura, *Appl. Phys. Lett.* ***70*** , 981-983 (1997).

[17] S Nakamura, M Senoh, S Nagahama, N Iwasa, T Yamada, T Matsusita, Y Sugimoto, H Kiyoku, *Appl. Phys. Lett.* ***70*** , 2753-2755 (1997).

[18] F.A. Ponce, S.A. Galloway, D. Cherns, W. Gotz, R.S. Kern. "Microstructure and spatial variation of luminescence in $In_xGa_{1-x}N$ quantum wells", Proc. of the Second Int. Conf. on Nitride Semicon. Oct 1997, Tokushima, Japan. p. 26

[19] A. I. Ekimov, F. Hache, M. C. Schanne-Klein, D. Ricard, C. Flytzanis, I. A. Kudryavtsev, T. V. Yazeva, A. V. Rodina, Al. L. Efros, *J. Opt. Soc. Am. B* ***10*** , 100-7 (1993).

[20] C Wetzel, T Takeuchi, H Amano, I Akasaki, unpublished.

[21] C Wetzel, T Takeuchi, S Nitta, S Yamaguchi, H Amano, I Akasaki, unpublished.

[22] C Wetzel, T Takeuchi, S Yamaguchi, H Katoh, H Amano, I Akasaki, *Appl. Phys. Lett.* ***73*** , 1994-6 (1998).

[23] C Wetzel, T Takeuchi, H Amano, I Akasaki, unpublished.

[24] H. Amano, T. Takeuchi, S. Sota, H. Sakai, I. Akasaki, *Mater. Res. Soc. Symp. Proc.* ***449*** , 1143 (1997).

[25] T Takeuchi, H Takeuchi, S Sota, H Sakai, H Amano, I Akasaki, *Jpn. J. Appl. Phys.* ***36*** , L177 (1997).

[26] A. Fischer, H. Kuhne, H. Richter, *Phys. Rev. Lett.* ***73*** , 2712 (1994).

[27] J. W. Matthews, A. E. Blakeslee, *J. Cryst. Growth* ***32*** , 265 (1976).

[28] M. Yamaguchi, T. Yagi, T. Azuhata, T. Sota, K. Suzuki, S. Chichibu, S. Nakamura, *J. Phys. C* ***9*** , 241 (1997).

[29] AF Wright, *J. Appl. Phys.* ***82*** , 2833-2839 (1997).

[30] L. Bellaiche, A. Zunger, *Phys. Rev. B* ***57*** , 4425 (1998).

[31] A Shikanai, T Azuhata, T Sota, S Chichibu, A Kuramata, K Horino, S Nakamura, *J. Appl. Phys.* ***81*** , 417-424 (1997).

[32] H. Sato, T. Sugahara, Y. Naoi, S. Sakai. "Compositional inhomogeneity of InGaN Layers grown on bulk GaN and sapphire substrates by MOCVD", Proc. of the Second Int. Conf. on Nitride Semicon. Oct 1997, Tokushima, Japan. p. 28

[33] D. Leonard, M. Krishnamurthy, C. M. Reaves, S. P. DenBaars, P. M. Petroff, *Appl. Phys. Lett.* ***63*** , 3203-5 (1993).

[34] S. Ruvimov, Z. Liliental-Weber, J. Washburn, H. Amano, I. Akasaki, M. Koike, *Mater. Res. Soc. Symp. Proc.* ***482*** , 387 (1998).

[35] R Singh, D Doppalapudi, TD Moustakas, LT Romano, *Appl. Phys. Lett.* ***70*** , 1089-1091 (1997).

[36] K. Osamura, S. Naka, Y. Murakami, *J. Appl. Phys.* ***46*** , 3432 (1975).

[37] N. A. El-Masry, E. L. Piner, S. X. Liu, S. M. Bedair, *Appl. Phys. Lett.* ***72*** , 40 (1998).

[38] I. H. Ho, G. B. Stringfellow, *Mater. Res. Soc. Symp. Proc.* ***449*** , 871 (1997).

[39] C. Wetzel, T. Takeuchi, H. Amano, I. Akasaki, *J. Cryst. Growth* ***189/190*** , 621-624 (1998).

[40] C Wetzel, H Amano, I Akasaki, T Suski, JW Ager, ER Weber, EE Haller, BK Meyer, *Mater. Res. Soc. Symp. Proc.* ***482*** , 489-500 (1998).

[41] D. E. Aspnes, *Phys. Rev. B* ***10*** , 4228 (1974).

[42] D. E. Aspnes, *Phys. Rev.* ***153*** , 972 (1967).

[43] T. L. Tansley, C. P. Foley, *J. Appl. Phys.* ***59*** , 3241 (1986).

[44] M. D. McCluskey, C. G. Van de Walle, C. P. Master, L. T. Romano, N. M. Johnson, *Appl. Phys. Lett.* ***72*** , 2725 (1998).

[45] Shuji Nakamura, Naruhito Iwasa, Shin-ichi Nagahama, *Jpn. J. Appl. Phys.* ***32*** , L338-L341 (1993).

[46] Shuji Nakamura , *J. Vac. Sci. Technol. A* ***13*** , 705-710 (1995).

[47] Shuji Nakamura, Gerhard Fasol, *The Blue Laser Diode - GaN based Light Emitters and Lasers* , (Springer-Verlag, Heidelberg, 1997), .

[48]

[49] B. K. Meyer, D. Volm, A. Graber, H. C. Alt, T. Detchprohm, A. Amano, I. Akasaki, *Sol. St. Comm.* ***95*** , 597 (1995).

[50] T. Takeuchi, S. Sota, M. Katsuragawa, M. Komori, H. Takeuchi, H. Amano, I. Akasaki, *Jpn. J. Appl. Phys.* ***36*** , L382 (1997).

[51] T Takeuchi, C Wetzel, S Yamaguchi , H Sakai, H Amano, I Akasaki, Y Kaneko, S Nakagawa, Y Yamaoka, N Yamada, *Appl. Phys. Lett.* ***73*** , 1691-3 (1998).

[52] A. D. Bykhovski , V. V. Kaminski , M. S. Shur , Q. C. Chen, M. A. Khan , *Appl. Phys. Lett.* ***68*** , 818-819 (1996).

[53] S. Shur in Compound Semiconductors Spring I (1998) p.12

[54] F. Bernardini, V. Fiorentini, D. Vanderbilt, *Phys. Rev. Lett.* ***79*** , 3958 (1997).

[55] A. Zunger *private communication*

[56] C. Wetzel, T. Takeuchi, H. Kato, H. Amano, I. Akasaki, "Piezoelectric effects in GaInN/GaN heterostructures and quantum wells", 24th Int. Conf. on the Physics of Semiconductors, Jerusalem, Israel, August 2-8, 1998. (World Scientific, Singapore 1998)

FIGURES

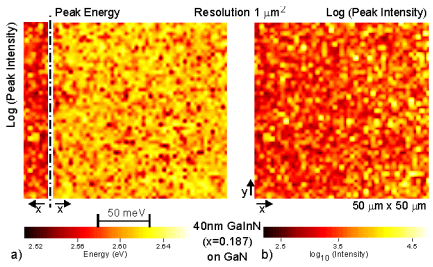

Figure 1. Spatially resolved PL mapping of an area of 50 ×50 μm^2 (T=300 K). a) Peak energy, b) peak intensity. A portion of the intensity map has been flipped and arranged next to the energy map. A spatial fluctuation in peak energy directly corresponds to a variation in intensity. Intensity is highest for high emission energy.

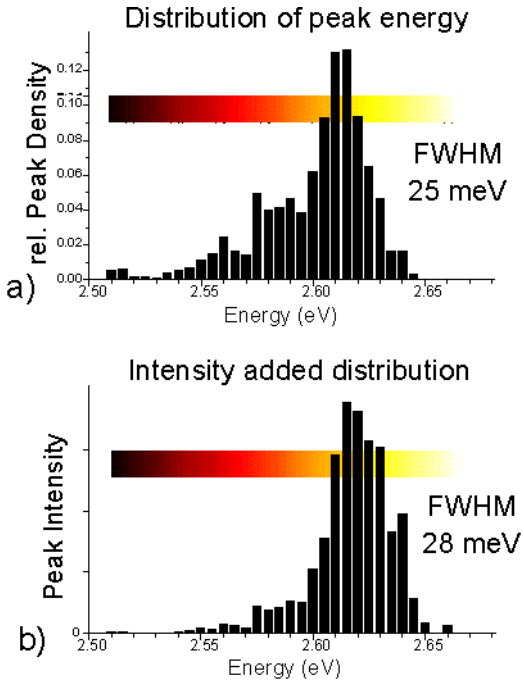

Figure 2. Energy distribution of maximum PL emission. a) Fraction of areal occurrence, b) same, weighed by its relative peak intensity. The scale for the coded energy is identical to Fig. 1. Luminescence peak energies show a very narrow distribution in energy. Lower energy peak emissions are irrelevant when their relative intensity is taken into account. The brightest emission occurs in the high-energy end of the distribution.

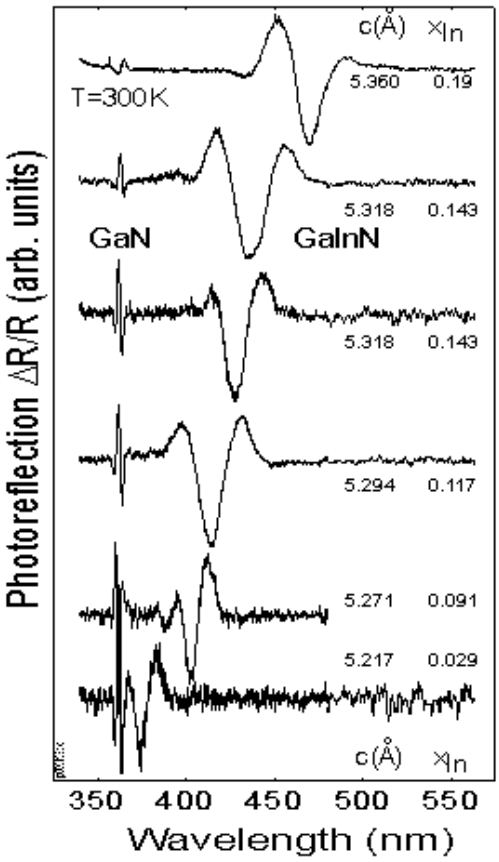

Figure 3. Photoreflection of the stressed GaInN/GaN layers as a function of composition. Measured c-lattice constants and interpreted x-values are indicated. In contrast to the narrow excitonic signal at the GaN bandedge, a very broad oscillation is seen at the GaInN band gap. The PR DOS band gap is associated with its dominant minimum.

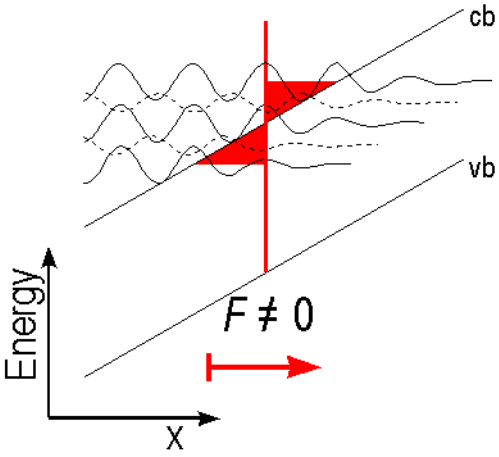

Figure 4. Schematic of the electronic bandstructure in the presence of a large electric field F. Due to reflection at the inclined conduction band edge states in the conduction band establish a phase correlation in energy in the location of the interband transition indicated by the red line (Franz-Keldysh oscillations). Below the band gap energy evanescent waves contribute at an exponentially decaying rate controlled by the tunneling probability given by the area of the lower shaded triangle (Franz-Keldysh effect).

MRS Internet J. Nitride Semicond. Res. 3, 31 (1998).

https://doi.org/10.1557/S1092578300001034 Published online by Cambridge University Press

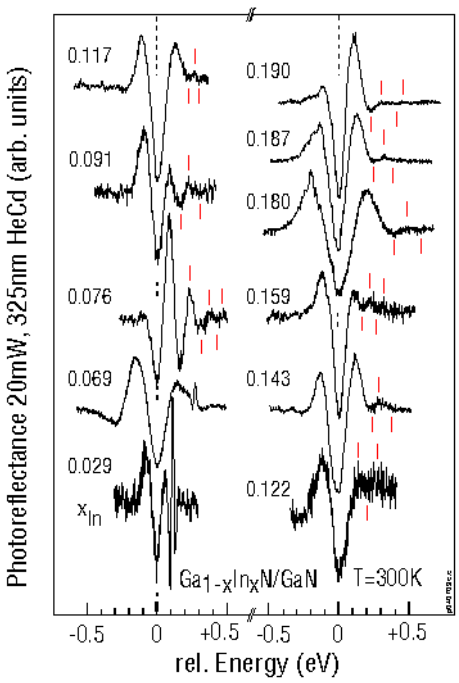

Figure 5. PR signal in the vicinity of the GaInN band gap. All spectra show subsidiary oscillations on the high energy side. Extrema are indicated by ticks. The period of these Franz-Keldysh oscillations is a direct measure of the electric field acting across the GaInN layer.

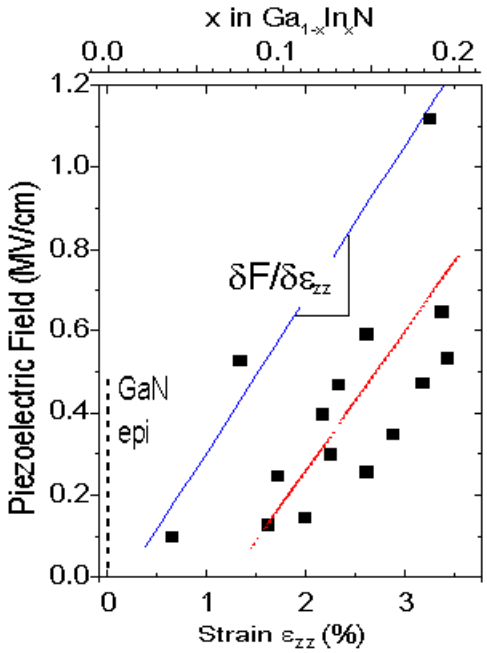

Figure 6. Derived electric field values as a function of strain and composition. A maximum field of 1.12 MV/cm is identified. The strain condition of the GaN layer is taken as a reference. F in the large number of samples follows a common slope. Two sub sets approximated by the red and blue lines exhibit finite and vanishing offsets, respectively.

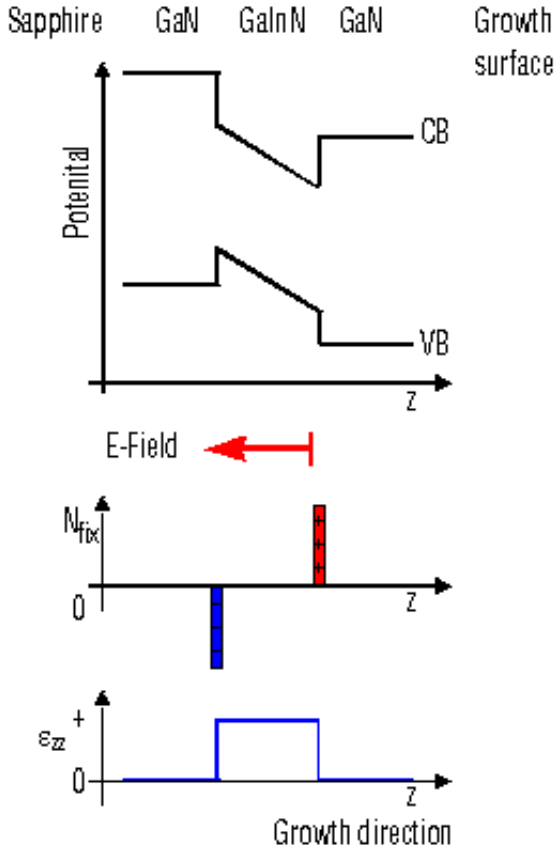

Figure 7. Schematic of the strain induced along the growth direction, the resulting δ-layers of fixed piezoelectric charges, and the resulting bandstructure for a GaN-GaInN-GaN heterostructure. The proper direction of the electric field found in our growth process is indicated as derived in Ref. [51] .

https://doi.org/10.1557/S1092578300001034 Published online by Cambridge University Press

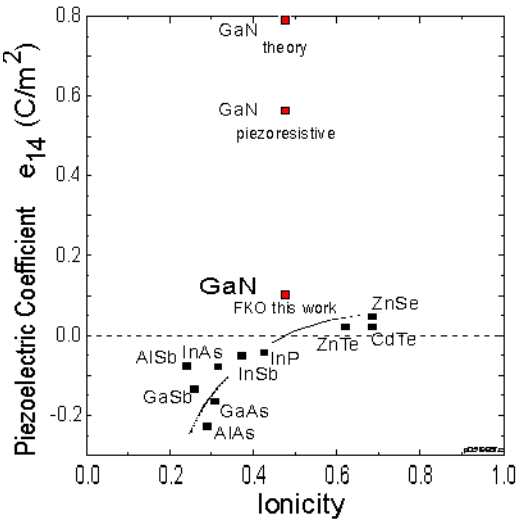

Figure 8. Cubic and quasi-cubic piezoelectric coefficient e_{14} in various compound semiconductors versus their ionicity. Our value derived for GaN lies within the trend while results from piezoresistivity [52] and first principles calculations [54] show significantly higher values. After Ref. [53].

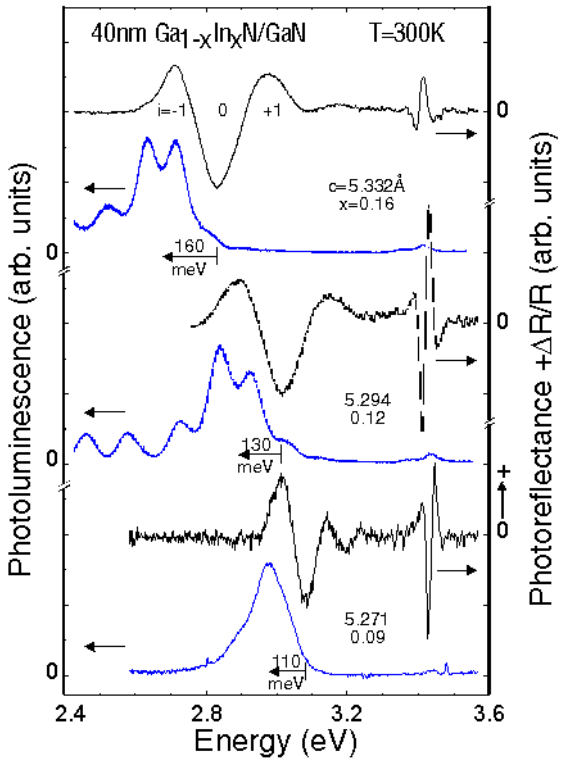

Figure 9. PR and corresponding PL of thin film GaInN/GaN single heterostructures. With increasing x, ε_{zz}, and F the splitting of the dominant PR minimum i=0 and the PL maximum increases. The PL maximum closely coincides with the i=-1 maximum. We attribute this splitting to the Franz-Keldysh effect.

MRS Internet J. Nitride Semicond. Res. 3, 31 (1998).

https://doi.org/10.1557/S1092578300001034 Published online by Cambridge University Press